DEVELOPMENT OF A SIMULATION-BASED DECISION SUPPORT TOOL FOR RENEWABLE ENERGY INTEGRATION AND DEMAND-SUPPLY MATCHING

Born F J, Clarke J A and Johnstone C M
Energy Systems Research Unit
Department of Mechanical Engineering
University of Strathclyde
Glasgow G1 1XJ
esru@esru.strath.ac.uk

ABSTRACT

This paper describes a simulation-based decision support tool, MERIT, which has been developed to assist in the assessment of renewable energy systems by focusing on the degree of match achievable between energy demand and supply. Models are described for the prediction of the performance of PV, wind and battery technologies. These models are based on manufacturers' specifications, location-related parameters and hourly weather data. The means of appraising the quality of match is outlined and examples are given of the application of the tool at the individual building and community levels.

INTRODUCTION

Recent political shifts towards greater renewable energy (RE) utilisation has resulted in RE technologies being utilised at two levels: large scale systems integrated into the electricity supply infrastructure (i.e. distributed generation); and small scale systems integrated with a building's electricity supply network (i.e. embedded generation). In the former case, it is estimated that capacities of up to 25% of maximum demand can be accommodated before technical difficulties begin to occur with the management and operation of the supply network. In the later case, to prevent network problems being created, the approach being adopted is to utilise the RE-derived power to displace the power that would otherwise be taken from the local supply network. Since the RE technologies being developed for building integration are stochastic, this creates problems for mechanical and electrical design in relation to

- the selection of technology types and capacities, and physical size of the RE system to be installed;
- local utilisation of the variable power delivered throughout the year; and
- satisfying the likely requirement for, and capacity of, energy storage if export is to be avoided.

A simulation-based, decision-support tool has been developed as part of an EPSRC research project (Clarke *et al*. 2001) addressing the impact of embedded generation on a building's energy performance and the ability of the approach to displace demands exerted on the public electricity supply network.

SYSTEM ARCHITECTURE

The MERIT system (Born 2001) has been developed in Visual C++ as a multiple-document application within which linked windows relate to the different aspects required to define a supply/demand matching study: namely, the specification of weather and simulation period parameters, demand profiles, fuel supply systems (e.g. anaerobic digestion, fermentation etc) and RE/auxiliary power delivery systems.

Figure 1 depicts the system framework; which uses open database connectivity to communicate with a remote SQL database via the Internet. This enables data exchange with other energy analysis tools, for example:

- building simulation tools can be used to provide virtual demand profiles relating to scenarios for which there are no real data;
- energy monitoring and targeting software supports the analysis of time series data corresponding to the consumption of fuel and power at the individual meter level; and
- GIS software can access the database and present energy supply/demand matching data enabling further RE systems analysis based, for example, on environmental sensitivity.

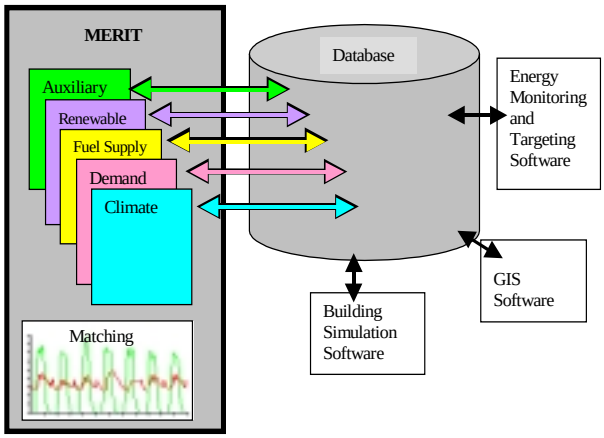

Figure 1: The MERIT framework.

RE SYSTEMS SIMULATION

RE systems algorithms have been developed to simulate power production based on manufacturers' specifications, locational parameters and weather data.

Crystalline Photovoltaic Devices

Different PV modelling techniques are available, which can be used to determine a specific PV system's supply profile. Detailed models developed for cell design purposes (Maotro and Araujo 1997) are not suitable here as they require specialised input parameters not readily available. Because the electrical behaviour of a PV system is highly dependent on incidental solar flux and thermal parameters, models solely based on equivalent electrical circuits (Katan *et al* 1995) are not capable of determining variations in supply profiles resulting from changes in system configurations, e.g. encapsulation and hybrid applications. Other approaches, based on curve-fitting techniques (Russell 1994, Kelly 1998) determined through experimentation, are not generic in nature.

The model as implemented is based on a consideration of solar geometry to calculate the angle of incidence of solar radiation on the PV surface (Duffie and Beckman 1974). To estimate the surface radiation balance, absorption, reflection and transmission coefficients are required as a function of angle of incidence. Experiments have shown that coefficient dependence on wavelength is relatively weak for a typical PV module (Preu *et al* 1995). By neglecting this dependence, it is possible to quantify the fraction of solar radiation absorbed in the silicon layer. A thermal energy balance model is then employed to evaluate the panel temperature, which directly affects the power capacity of the cell. Finally, an equivalent electrical model is used to determine the supply.

A linear correlation exists between increases in PV cell temperature and reduction in open circuit voltage, which in turn reduces the power output. A temperature increase from 40°C to 150°C can reduce the power output by 60% (Decher 1997). To quantify the electrical output from a PV system it is therefore vital to predict the panel temperature. PV-hybrid systems recover heat from the module, reducing the panel temperature and simultaneously producing a source of low grade thermal energy. The heat available from hybrid systems can subsequently be used in assessing the match between thermal supply and demand. If a hybrid system is specified, the radiant exchange with the back wall, and convective heat losses from the panel to the air gap are considered. When modules are configured without heat recovery these terms are omitted, leaving only the radiation exchanges with the sun and sky, convective heat losses due to wind conditions, and heat loss through power extraction, to be considered. The first stage of the process involves the use of the Newton-Raphson method to solve an energy balance equation:

$$m \cdot c \cdot \Delta T = Q_s - \frac{A \cdot \sigma \cdot \left(T^4 - T_{wall}^4\right)}{\frac{1}{\varepsilon} + \frac{1}{\varepsilon_{wall}} - 1} - \varepsilon \cdot A \cdot VF \cdot \sigma \cdot \left(T_{sky}^4 - T^4\right) - A \cdot h_{wind} \cdot \left(T_a - T\right) - A \cdot h_g \cdot \left(T_a - T\right) - Q_{pow}$$

where m is the mass of the silicon layer (kg), c the specific heat of silicon (J/kgK), ΔTthe change in panel temperature (K), T_a the ambient temperature (K), T_{sky} the sky temperature (K), T_{wall} the temperature of the wall (K), Q_S the radiant exchange with the wall (W), Q_{pow} the heat removed in power production (W), ε the emissivity of the PV backing, ε_{wall} the emissivity of the wall, A the surface area of PV (m^2), VF the view factor, σ the Stephan Botzmann constant (5.669 x 10^{-8} W/m^2-K^4), h_{wind} the convective heat transfer coefficient (W/m^2K) and h_g the gap convective heat transfer coefficient (W/m^2K).

The second stage involves the use of an equivalent electrical circuit to model the electrical output from a PV cell, where the

- p-n junction is represented by a current source, whose output is dependent on the photon flux;
- the current through the diode is used to represent recombining hole and electron pairs, which reduces the output from the cell;

- cells internal resistance is in series with the load resistance; and
- the shunt in parallel with the p-n junction is the intrinsic self-shortening of the cell, which for silicon cells is usually small enough to be negligible.

The inclusion of the shunt resistance enables the modelling of amorphous cells (Fry 1998). This equivalent circuit is used to evaluate the dark and source currents, which enables the power output from a cell to be predicted.

In the absence of a photon flux reaching the p-n junction, a current is established, known as the dark current, I_o, which is defined as (Decher, 1997):

$$I_o = 4 \cdot \left(\frac{2 \cdot \pi \cdot e \cdot m_e}{h^2} \right)^3 \cdot \left(\frac{\mu_h \cdot \mu_e}{L_h \cdot \sigma_e} \right) \cdot \left[\left(\frac{k \cdot T}{e} \right)^4 \cdot \exp\left(\frac{e \cdot V_g}{K \cdot T} \right) \right]$$

where e is the electron charge (1.602 x 10-19 Coulomb), m_e the electron mass (9.109 x 10-31 kg), h Planck's constant (6.626 x 10-34 kg), μ_h the hole diffusion velocity, μ_e the electron diffusion velocity, σ_e the electrical conductivity for electrons, V_g the band gap (1.1 eV for silicon), k Boltzmann's constant (1.381 x 10-23 J/K) and T the cell temperature (K).

Since specific material property parameters required for dark current evaluation (e.g. hole and electron diffusion velocities) are typically not available, a single material parameter can be established from the manufacturers' performance data at standard test conditions (STC), i.e.1000W/m^2 irradiation and 25ºC cell temperature. Since source current is linearly dependent on the absorbed solar radiation and module temperature this linear relationship can be used in the evaluation process. Since the intensity of solar radiation available at the p-n junction at STC and operating conditions will be different, it is necessary to quantify losses in intensity in order to make use of the linear current-radiation relationship. The source current density, in the case of silicon, is known to increase with temperature at a rate of 10^{-4}A.m^{-2}K^{-1} (Decher 1997). This figure has been used to account for changes in current resulting

$$I_S = \left(\frac{I_{STC} \cdot Q_{STC} \cdot R(0)}{Q \cdot R} \right) + I_{STC} \cdot A_p \cdot (T - T_{STC}) \cdot 10^{-4}$$

from a deviation in the STC temperature. The following equation is used to predict the source current for silicon cells.

where I_{STC} is the short circuit current at STC, Q_{STC} the STC irradiance, R(0) the reflection losses at zero incidence, Q the predicted solar radiation, R the predicted reflection losses, T the predicted panel temperature, T_{STC} STC temperature and A_p the module area.

The load current and voltage across the external load is calculated using the following equations.(Decher 1997):

The power output is always calculated for the PV

$$I = I_S - I_j = I_S - I_o \cdot \left[\exp\left(\frac{e \cdot V_g}{K \cdot T} \right) - 1 \right]$$

$$V = V_{OC} \cdot \frac{\ln\left(1 + \left(1 + \frac{I}{I_O} \right) \cdot \frac{I_S}{I_O} \right)}{\ln\left(1 + \frac{I_S}{I_O} \right)}$$

system operating at its maximum power point. This assumption is reasonable as building-integrated PV systems nearly all employ a maximum power point tracker (Fry 1998). An implicit expression for the ratio of supply current to the dark current is solved using the Newton-Raphson technique to provide a solution for the current flowing through a particular load resistance. The corresponding voltage is calculated from the fill factor, which enables the power output from a single cell to be determined. This is scaled according to the module configuration and the number of modules contained within a system. Typically, a PV system will be operating in conjunction with an inverter. A detailed electrical model of the inverter, which accounts for the switching losses and device impedance, requires information that is not readily available. Consequently, an approximation has been incorporated based on a typical inverter performance curve. The approximation accounts for the losses in efficiency at low percentage loading.

Wind Energy Conversion Devices

The primary objectives in modelling wind systems are similar to PV: the model should be applicable to a variety of wind energy conversion systems; and the inputs to the model should be obtainable from manufacturers' specifications. Accurate and reliable prediction of a wind turbine's aerodynamic performance requires detailed data about wind flow, aerodynamic profile and turbine design, to account for the many factors impacting on performance. Detailed models exist (Muljadi *et al* 1998) to predict high and low speed shaft torques as a function of time. However, these models require data such as blade geometry, rotor inertia, drive-train inertia, and stiffness and damping of the rotating shafts. The drive train stiffness of a particular turbine dictates whether dynamics need to be included, and the pitch actuation system used will

determine the actuator dynamics (Pierce and Fingersh 1998). The requirement to model performance based on manufacturers' data and climate parameters constrain the approach by neglecting the fundamentals of detailed aerodynamic performance. Oversimplified approaches are also unsuitable, such as considering only rated power production for wind speeds with sufficient velocity, and neglecting any power production in the run up to rated power (Enslin and Potgieter 1996), or calculating power output assuming a constant coefficient of performance (Ramirez 1998).

The approach adopted in MERIT (Child *et al* 1996) calculates power output using a turbine's empirical wind power curve as a look-up table. This method is employed for all but ducted wind devices (Webster 1979) for which no manufacturers' data exists.

A number of parameters, which are independent of the turbine type are required in the performance calculations including blade swept area, turbine (hub) height and the reference air density used by manufacturers to produce the empirical power curve. All parameters can be obtained from power curves, with the exception of a ducted wind turbine where turbine orientation is the only input parameter required.

Wind speed data is corrected for surrounding surface roughnesses and proposed turbine height (Troen and Petersen 1991). These corrected wind speeds are used to estimate corresponding power outputs, which are then corrected to account for air density variations. This correction is based solely on temperature variations assuming constant atmospheric pressure.

The algorithm developed to predict the performance of ducted wind turbines was derived from an analysis of field trial data and obtained for a prototype tested at the National Wind Turbine Test Centre (Grant *et al* 1994). These data show the power output to be dependent on both wind speed and wind direction. A correction factor was evaluated to include the effects of wind angle of incidence on power output. Increases in angular incidence reduce power outputs, with angles greater than 75 degrees resulting in the cessation of power production. The magnitude of the reduction in power output is also proportional to the wind speed. The correction factor for misalignment was applied to the wind speed to obtain an expression for power as given in the following equation. Clearly, the kinetic energy in the wind available at the rotor swept area is proportional to the angle of incidence, with obtuse angles reducing the wind power at the rotor. For zero angles of incidence the wind speed at the rotor is the actual wind speed, and as the angle increases the effective wind speed is reduced.

where V_c is the corrected wind speed at the rotor, V_w the wind speed, θ the angle of misalignment, and θ_{max}

$$V_C = V_w \cdot \left(1 - \frac{\theta}{2 \cdot \theta_{max}} \right)$$

the maximum angle of misalignment (75 degrees).

The power of the wind at the rotor can be calculated from

$$P_w = \frac{1}{2} \cdot \rho \cdot A \cdot V_C^3$$

where P_w is the power of the wind at the rotor (W), ρ the density of air (kg/m3), A the rotor swept area (m^2), $V_c$the corrected wind speed (m/s).

Regression analysis performed on the calculated power in the wind at the rotor, and the power output from the turbine, was used to ascertain the relationship between these two power characteristics, which essentially describes a function of the coefficient of performance, Cp. The regression polynomial from this analysis was valid for corrected wind speeds up to approximately 22m/s. Corrected wind speeds greater than this could be seen to increase the power output from the turbine in a linear manner.

The analysis described gave rise to the following modelling technique used to predict the power output from a ducted wind turbine. Firstly, any wind incidence angles greater than 75 degrees result in zero power output. Provided the angle of incidence is within this upper limit, the wind speed is corrected to account for misalignment and this effective wind speed is used to calculate the power in the wind at the rotor. For wind powers less than the limiting value of 3.5 kW, the turbine power output is determined from

$$P_t = 0.0007 \cdot P_w + 66.396$$

while for other conditions, it is determined from

$$P_t = 0.030897 \cdot P_w + 0.2285$$

where P_t is the power output of the turbine (W) and P_w the power of the wind at the rotor (W)

Powers exceeding the limiting value are due to conditions of significant turbulence being induced, which inhibits the ability of the turbine to extract the power available.

STORAGE SIMULATION

In order to assess the impact of storage on the ability of a renewable energy system to meet demand, a model for a lead-acid rechargeable battery was developed.

Detailed models examining the various electro-chemical and physical processes occurring within batteries (Newman and Tiedemann 1997, Notten *et al* 1998) require specific data not normally provided by manufacturers. Other models based on over-simplified assumptions, e.g. constant discharge efficiency (Child *et al* 1996), require the determination of empirical values through laboratory testing (Protogeropoulos *et al* 1994, Morgan *et al* 1997). The battery model developed in this work is generic, is based on manufacturers' data and assumes the battery system to be operating in conjunction with a charge regulator whose function is to regulate both the charging voltage and current to prevent battery damage.

The power delivered or absorbed by a battery is dependent on its open circuit voltage, the discharge/ charge current and the internal resistance. This model is based on the relationship between open circuit voltage and state of charge of a single cell. Typical open circuit voltage and state of charge data was used to obtain a mapping function between these two parameters. A regression analysis of the published data led to the derivation of a 6th order polynomial function. As batteries consist of a number of series connected cells, the cell voltage may be scaled to represent any battery configuration.

During battery discharge, Thevinin's theorem (Davis 1992) is employed to convert the power required of the battery into a current. The level of charge stored in the battery will dictate whether the current requirement can be met. The charge stored in a fully charged battery is described by its capacity, which is a function of the discharge current. A battery will deliver less energy the quicker it is discharged. This phenomenon is the Peukert Effect, which describes declining capacity at increasing rates of discharge as a logarithmic curve (Ure 1998). Batteries can be described by their Peukert exponent values, which are directly related to the internal resistance of the battery. The relationship between battery capacity and rate of discharge is obtained from

$$C = A \cdot \ln(t) + B$$

where C is the battery capacity (Ahrs) and t the time to full discharge (hours). The constants A and B will vary with different battery configurations and internal resistances, and can be evaluated using two different capacity values (C1 and C2) specified for different discharge rates (t1 and t2).

The process for calculating the charge stored within the battery assumes the battery is fully charged initially and its capacity for any given discharge current known. To determine the actual charge, the capacity for a given discharge current is multiplied by the percentage state of charge. Knowing the charge to be supplied and the charge stored in the battery, the resultant charge to be supplied can be calculated. This resultant charge is compared to the charge at a specified deep discharge level to determine whether the battery charge control system will allow this rate of discharge current. Where the resultant charge is less than the battery's deep-discharge rating, an iterative process is initiated that gradually decreases the discharge current requirement to a level the battery is capable of supplying without discharging below the deep discharge level. The power dissipated to the load, P, is calculated using the following equation with the resulting state of charge mapped to the corresponding open-circuit voltage.

$$P = I \cdot V - I^2 \cdot r$$

Battery charging is modelled assuming the use of a charge regulator designed to prevent overcharging and according to the phase of charge. The bulk-charging phase is modelled by assuming the maximum charging current is supplied to a battery when its state of charge is below 75%. No distinction is made between absorption and float charge phases, and the charging current is modelled as a decreasing exponential as the battery's ability to accept charge is reduced:

Where I_c is the charging current required at time t(A),

$$I_C = I_{max} \cdot e^{-t}$$

I_{max} the maximum charging current (A), t the time for the current to decay from I_{max} to I_c (hrs).

In order to predict the charge accepted by a battery, the current at the beginning and end of a charging interval must be evaluated. To do this two assumptions are made: the charge stored in a fully charged battery is assumed to be that of the battery's capacity rated at 20 hours; and the charge required at the beginning of the charging period is assumed to be that required to recharge the battery fully within the given charge interval. Substituting this ideal charging current into the previous equation, enables the corresponding charge time to be established as a function of the change in charge, ΔQ:

The current available for battery charging can be found by solving I. Where the current available is less than that required, it is assumed that all the charge delivered

$$\Delta Q = \int_{t}^{t+1} I dt = \left[- I_{\max} \cdot \exp(-t2) + I_{\max} \cdot \exp(-t1) \right] \cdot \Delta t$$

is accepted. Where the current is greater than that required, only the proportion required is used, thereby assuming a charge controller is being used. The state of charge after charging is calculated as a percentage of the fully charged condition, and a mapping function is used to determine the open-circuit voltage. The power used, in charging the battery may then be calculated.

Other factors influencing battery performance include: self discharge, depth of discharge, temperature and battery configurations. Assuming the rate of self discharge specified by manufacturers to be linear, effects of self discharge can be incorporated when the battery is neither charging nor discharging.

Operating temperatures can affect a battery's performance in a number of ways. Accounting for temperature effects is further complicated by the size of a battery bank (i.e. its thermal mass) and any insulation used to protect a battery from temperature fluctuations. The effect of temperature on battery capacity is assumed to be linear between temperatures of -20°C and 20°C and also between 20°C and 60°C, but at different rates. These linear temperature effects are applied to the two rated capacities used to define a battery, at the beginning of every time-step calculation. Since these capacities are subsequently used in modelling all modes of battery operation, any temperature effects are accounted for. Battery discharge rates are evaluated utilising rated capacities. Battery state of charge is modelled as a percentage of the fully charged capacity, rated at 20hrs, to which temperature effects are applied. The state-of charge is mapped to battery voltage, which ensures temperature effects on voltage are incorporated. Battery charging currents are assumed to be unaffected by temperature since temperature compensation is included in the majority of battery charge control systems. However the effect of applying a certain charging current over a period of time will vary depending on temperature, as the amount of charge stored by the battery varies with temperature. Finally, self-discharge is modelled as a percentage reduction in capacity, therefore any percentage change in a temperature-affected capacity will account for any effects in self discharge.

This analysis relates to a single battery. For battery banks, including multiple batteries connected in series or parallel, standard electrical circuit theory is employed to model the effects of configurations. Identical batteries connected in series maintain the same capacity as a single battery. The total internal resistance is the sum of the internal resistances of the batteries and the total open-circuit-voltage is the sum of the open-circuit voltages. Connecting secondary cells in parallel in theory leads to greater current capacity. In practice, however, poor current sharing during both charging and discharging can occur. The effects of this phenomenon are not accounted for and parallel batteries are modelled theoretically. This results in the same open-circuit voltages as a single battery, a total capacity equal to the sum of the capacities and a reduced internal resistance.

MATCH ASSESMENT

The matching of supply options to demand profiles, explores the extent to which RE technologies can satisfy demand and identifies the storage capacity required to improve the match.

MERIT reports the match both graphically and with the use of statistical indices. It has the facility to conduct an automated search in order to identify those combinations that best match user-specified search criteria. The automated search facility activates data processing techniques which numerically assess the demand and supply, while excluding auxiliary systems data, in order to performance benchmark each match via a match assessment. Following this, a search ordering process presents the possible matches in order from best to worst.

The statistical indices used in assessing the match include Spearman's Rank Correlation Coefficient [Scheaffer and McClave 1982] to establish the phase matching between the demand and supply streams and an inequality coefficient described by Williamson [1994] to ascertain the magnitude of match. The Spearman's Rank Correlation Coefficient describes the correlation between the demand and supply variables by calculating the degree to which the variables fall on the same least square line. Calculation of this coefficient will result in a value between -1 and 1. A result of 1 indicates perfect positive correlation and -1 perfect negative correlation, i.e. as one variable tends to increase the other will decrease at the same rate. A value of zero denotes no correlation between the variables. The coefficient is used to describe the trend between the time series of two data sets and does not consider the relative magnitudes of the individual variables. Thus, if a supply system were doubled in size the correlation coefficient would remain the same even though the excess supply would be far greater. Additionally, two profiles perfectly in phase with one another, but of very different magnitudes, would result in a perfect correlation, but not a perfect match. Nevertheless, it provides a measure of the potential match, which could exist given changes to the relative capacities, i.e. through energy efficiency, demand side control or altering the size of the RE system.

The Inequality Coefficient, IC, describes the inequality in the magnitude domain due to three sources: unequal tendency (mean), unequal variation (variance) and imperfect co-variation (co-variance):

$$IC = \frac{\sqrt{\frac{1}{n}\cdot\sum_{t=0}^{n}(D_t - S_t)^2}}{\sqrt{\frac{1}{n}\cdot\sum_{t=0}^{n}(D_t)^2} + \sqrt{\frac{1}{n}\cdot\sum_{t=0}^{n}(S_t)^2}}$$

The resultant coefficient can range in value between 0 and 1, with 0 indicating a perfect match and 1 denoting no match. This metric is well suited to establishing bands of match, where matches resulting in inequalities between 0 and 0.1 could be termed good and bad matches are those resulting in values between 0.9 and 1.

The automated search facility is based on an exclusive search of all possible combinations of selected supplies and demands, and a search ordering process is conducted to identify which profile combinations are best (Born *et al* 2001).

FUTURE DEVELOPMENTS

MERIT is suitable for both macro (national, regional) and micro (community, institutional, individual building) level analysis. An example of system use at the micro level is the Lighthouse Building in Glasgow where a number of co-operating RE technologies have been deployed and their performance monitored (Born *et al* 2001). This design approach focused on the deployment of passive renewable technologies to both reduce energy requirements and reshape the demand profile, and active renewable technologies to meet a significant portion of the residual demand. The use of daylight together with smart lighting control resulted in an 81% reduction in lighting energy requirements. Heating requirements were reduced by 59% using transparently insulated façade components to achieve solar capture and time shift to off-set heating loads, together with advanced glazing to reduce heat loss and smart heating control. The active RE systems were then able to meet approximately 68% of the building's total energy demand.

On the macro level, MERIT is currently being used within the EC RESPIRE project aiming to establish mechanisms to progress towards 100% RE supply for remote and island communities. The methodology developed for achieving this will undergo robustness testing in five European island case studies where high RE penetration are being established. MERIT is being used to identify demand side measures, which can be implemented to reduce energy consumption and alter the demand profile to one more favourable to renewable technologies, for a case study on the Island of Islay situated off the south-west coast of Scotland. It is hoped that such an approach can increase the competitiveness and energy self-sufficiency of remote communities.

CONCLUSIONS

This paper has described the MERIT system developed to assist with the quantification of the match between RE supplies and demand, a critical issue in the assessment of intermittent sources of supply. Specifically, PV, wind turbine and battery models were described and a procedure for estimating the degree of match elaborated. MERIT can be applied at a variety of scales and has been designed to minimise the requirement for prior knowledge of the RE systems of interest.

REFERENCES

Born F J (2001), 'Aiding Renewable Energy Integration through Complimentary Demand-Supply Matching', PhD Thesis Strathclyde University

Born F J, Clarke J A and Johnstone C M (2001), 'Development and Demonstration of a Renewable Energy Based Energy Demand/Supply Decision Support Tool For the Building Design Profession' proceedings of BS2001, RIO.

Born F.; Clarke J.; Johnstone C.; Kelly N.; Burt G.; Dysko A.; McDonald J.; Hunter I. (2001), On the integration of renewable energy systems within the built environment, Building Services Engineering Research and Technology, vol. 22, no. 01, pp. 03-13

Child D., Smith I.R. and Infield D.G.(1996), Wind, Photovoltaic and Battery Electrical Power: Expeience and Modelling of an Autonomous and Grid Connected System, Int. Journal of Ambient Energy, Vol 17, No3.

Clarke J.A. Johnstone C.M. McDonald J and Burt G (2001) ' Maximising energy utilisation and power quality of supply in building-integrated renewable energy systems' EPSRC Grant GR/L77522 RA0744, UK.

Davis T. J. (1992), Circuit Calculations, Butterworth-Heinemann Ltd.

Decher R. (1997), Direct Energy Conversion, Oxford University Press

Duffie, J.A. and Beckman W. A. (1974), Solar Energy Thermal Processes, John Wiley & Sons, New York.

Enslin J.H.R. and Potgieter A. W. (1994), Computer Aided Design of Renewable Energy Systems. Elektron, Volume 8, issue 7.

Fry B. (1998), Simulation of Grid-Tied Building Integrated Photovoltaic Systems, Msc Thesis University of Wisconsin-Madison

Grant A.D., Nasr el-Din S.A., Kilpatrick J.(1994), Development of a Ducted Wind Energy Converter. Wind Engineering Volume 18 , Number 6, p.297-303.

Katan R. E., Agelidis V. G., Nayar C. V.(1995), PSPICE Modelling of Photovoltaic Arrays.

Kelly N. (1998), Towards a Design Environment for Building-Integrated Energy Systems: The Integration of Electrical Power Flow Modelling with Building Simulation, PhD Thesis Strathclyde University.

Maroto J.C. and Araujo G.L., (1997) Three-Dimentional Circuit Analysis applied to Solar Cell Modelling,

Morgan T. R., Marshall R. H., Brinkworth B. J.(1997), 'Ares' – A refined Simulation Program for the Sizing and Optimisation of Autonomous Hybrid Energy Systems, Solar Energy, Vol 59, No 4-6, pp 205-215.

Muljadi E., Pierce K and Migliore P. (1998), Control Strategy for Variable-Speed, Stall-Regulated Wind Turbines, American Controls Conference.

Newman J. and Tiedemann W. (1997), Simulation of Recombinant Lead-Acid Batteries, Journal of Electrochemical Society, Vol 144, No 9, pp.3081-3090.

Notten P.H.L., Kruijt W.S. and Bergveld H.J. (1998), Electronic Network Modelling of Rechargeable Batteries, Journal of Electrochemical Society, Vol 145, No 11, pp. 3774-3782.

Pendas I.A. (1999), Investigation of a Wind Energy Module. Final Year Project Thesis, University of Stathclyde.

Pierce K. and Fingersh L.J. (1998), Wind Turbine Control System Modelling Capabilities, American Controls Conference, Philadelphia, PA.

Preu R., Kleiss G., Reiche K. and Bucher K. (1995), PV-Module Reflection Losses: Measurement, Simulation and Influence on Energy Yield and Performance Ratio, 13th European Photovoltaic Solar Energy Conference.

Protogeropoulos C., Marshall R. H., Brinkworth B. J. (1994), Battery State of Voltage Modelling and an Algorithm Describing Dynamic Conditions for Long-Term Storage Simulation in a Renewable System., Solar Energy, Vol 53, No 6, pp 517-527.

Ramirez M. A. S. (1998), Electrification of a Saline Based Dwelling by Means of a Standalone Rural Energy System. M.Sc. Thesis, University of Strathclyde.

Russell Miles C. (1994), Grid-tied PV System Modelling: How and Why, WCPEC; Hawaii.

Scheaffer R.L. and McClave J.T. (1982), Statistics for Engineers, PWS Publishers.

Troen Ib, and Lundtang P. (2000): European Wind Atlas, Risoe National Laboratory, Risoe, Denmark, 1991, ISBN 87-550-1482-8, URL:http://www.risoe.dk/.

Ure G. (1998), App. Note: Why Batteries Shrink, www.cruisingequip.com/ftp/Battery%20Shrink.pdf

Webster G.W. (1979), Devices for Utilising the Power of the Wind, United States Patent 4152556.

Williamson T.J., (1994) 'A Confirmation Technique for Thermal Performance Simulation Models', University of Adelaide, Austrailia,.